[2] Liepmann, H. W., Ashkenas, H., and Cole, J. D., "Experiments in Transonic Flow," Tech. Rept. 5667, Feb. 1948, Air Force Air Material Command, Wright-Patterson Air Force Base, Ohio.

[3] Alber, I. E., Bacon, J. W., Masson, B. S., and Collins, D. J., "An Experimental Investigation of Turbulent Transonic Viscous-Inviscid Interactions," *AIAA Journal*, Vol. 11, No. 5, May 1973, pp. 620–627.

[4] Klineberg, J. M. and Steger, J. L., "Calculation of Separated Flows at Subsonic and Transonic Speeds," *Lecture Notes in Physics*, Vol. 19, Springer-Verlag, New York, 1972, pp. 161–168.

[5] Collins, D. J., "An Inexpensive Technique for the Fabrication of Two-Dimensional Wind-Tunnel Models," *Review of Scientific Instruments*, Vol. 44, No. 7, July 1973, p. 855.

[6] Collins, D. J. and Krupp, J. A., "Experimental and Theoretical Investigations in Two-Dimensional Transonic Flow," *AIAA Journal*, Vol. 12, No. 6, June 1974, pp. 771–778.

[7] Collins, D. J. and Krupp, J. A., "Experimental and Theoretical Investigations in Two-Dimensional Transonic Flow," AIAA Paper 73-659, Palm Springs, Calif., 1973.

Stretch Time of Scribed Metal Diaphragms

S. K. CHAN*
Institute for Aerospace Studies, University of Toronto, Toronto, Canada

Introduction

DIAPHRAGMS are commonly used in shock tubes as quick-opening valves to release the high-pressure driver gas into the low-pressure channel. Ideally the diaphragm should open fully instantaneously. In practice the diaphragm opens in two stages; namely, the stretching stage and the petaling stage, each of which takes a finite time. In a conventional shock tube, the exact time the diaphragm starts to open is not critical to the operation. Therefore, the stretch time is immaterial. However, the petaling time has a strong influence on the shock-formation processes.[1,2] It is possible to estimate the petaling time of a scribed metal diaphragm from a number of analyses.[3-5] Nevertheless, there does not appear to be a theory dealing with diaphragm stretching. The stretch time of a diaphragm is a very important factor in the operation of devices such as the free-piston shock tube[6] and the UTIAS implosion-driven shock tube.[7,8] In particular, the UTIAS implosion driver is a dynamic system for which the timing of the implosion wave to match the diaphragm opening is very critical in order to obtain the maximum possible shock velocity, from a given driver condition. Otherwise, some of the implosion energy is dissipated in opening the diaphragm. Therefore, it is very important to have an estimate of the diaphragm stretch time. In the following analysis, only scribed metal diaphragms are considered. It can, however, be applied equally well to nonmetalic diaphragms.

Analysis

Figure 1a shows a sketch of a sectional view of a typical scribed diaphragm. The diaphragm is divided into two layers, 1 and 2,

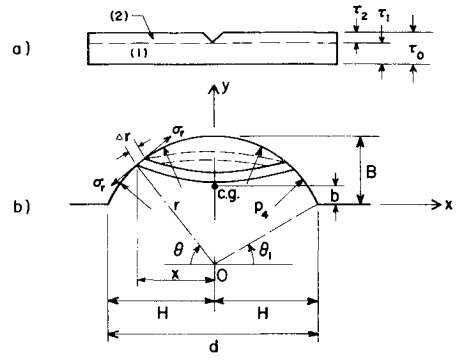

Fig. 1 Sketch of a section of the diaphragm and the stretching-diaphragm model.

with thickness τ_1 and τ_2, respectively. In the following analysis it is assumed that only Layer 1 exerts any resisting stress against stretching.

Consider an elemental ring with width Δr as shown in Fig. 1b. Pressure p_4 on the inside of the diaphragm exerts on the element a vertical force ΔF_p given by

$$\Delta F_p = 2\pi r^2 \cdot \cos\theta \cdot \sin\theta \, d\theta \cdot p_4 \tag{1}$$

The resultant vertical force ΔF_s due to circumferential stress σ_r on the two sides of the ring is given by

$$\Delta F_s = -2\pi\tau\sigma_r r \cdot \cos\theta \cdot \sin\theta \, d\theta \tag{2}$$

where τ is the instantaneous thickness of Layer 1 during the stretching process. The negative sign indicates a downward force. Apply Newton's second law to the vertical forces

$$\Delta F_p + \Delta F_s = \Delta m \, d^2y/dt^2 \tag{3}$$

where Δm is the mass of the elemental ring which includes the mass of Layer 2.

To obtain an estimate of stress σ_r we assume that the stretching diaphragm behaves as a section of a thin sphere with a uniform thickness. Equation (3) can then be integrated with r, τ, and σ_r a function of time t only

$$\int_{\theta_1}^{\pi/2} (\Delta F_p + \Delta F_s) = \int_{\theta_1}^{\pi/2} \Delta m \frac{d^2y}{dt^2} \tag{4}$$

where

$$\int_{\theta_1}^{\pi/2} \Delta F_p = \pi H^2 p_4 \tag{5}$$

and

$$\int_{\theta_1}^{\pi/2} \Delta F_s = -\pi \tau \sigma_r r \cos^2\theta_1 \tag{6}$$

with

$$\cos\theta_1 = 2BH/(H^2+B^2)$$
$$\tau = \tau_1 H^2/(H^2+B^2)$$

The right-hand side of Eq. (4) is simply

$$\int_{\theta_1}^{\pi/2} \Delta m \frac{d^2y}{dt^2} = \frac{d^2}{dt^2}\int_{\theta_1}^{\pi/2} \Delta m \cdot y = m\frac{d^2b}{dt^2} \tag{7}$$

where m is the total mass of the diaphragm and b is the distance of the c.g. of the bulging diaphragm from the base and $b = B/2$.

Substituting Eqs. (5–7) into Eq. (3) and letting $\eta = b/H$, after simplifying,

$$\frac{p_4}{\rho\tau_o H} - \frac{\tau_1}{\tau_o}\frac{\sigma_r}{\rho H^2}\frac{4\eta}{(1+4\eta^2)^2} = \frac{d^2\eta}{dt^2} \tag{8}$$

where ρ is the density of the diaphragm material. The stress-strain relationship in the plastic region can be represented by the usual form $\sigma_r = K\varepsilon_r^n$ where K is a stress proportionality constant and n is the strainhardening exponent. The tangential strain ε_r is related to the thickness strain ε_τ by the following

$$\varepsilon_1 + \varepsilon_2 + \varepsilon_\tau = 0 \tag{9}$$

Received December 19, 1973; revision received February 5, 1974. The work was financially supported by AFOSR (USA-AFOSR 72-2274B) and by NIC (Canada).

Index categories: Shock Waves and Detonations; Structural Dynamic Analysis.

* Graduate Student; presently Research Physicist at the Explosives Research Laboratory, Canadian Industries Limited, McMasterville, Quebec. Associate Member AIAA.

where

$$\varepsilon_1 = \varepsilon_2 = \varepsilon_r$$

Therefore

$$\varepsilon_r = -\varepsilon_\tau/2$$
$$= \tfrac{1}{2}[\tau/\tau_1 - 1] = \tfrac{1}{2}[4\eta^2/(1+4\eta^2)] \quad (10)$$

Substituting Eq. (10) into Eq. (8), after simplifying and integrating, we have

$$\left(\frac{d\eta}{dt}\right)^2 = \frac{2p_4}{\rho\tau_o H}\left[\eta - \frac{1}{2}\frac{\tau_1}{H}\frac{K}{p_4}\int_o^{\eta_B}\frac{(2\eta^2)^n\, d(1+4\eta^2)}{(1+4\eta^2)^2}\right] \quad (11)$$

If we further assume that the material behaves as a perfect plastic with $n = 0$ or $\sigma = K = \text{const}$, we can integrate Eq. (11)

$$dt = \left(\frac{\rho\tau_o H}{2p_4}\right)^{1/2}\frac{d\eta}{[\eta - \beta\eta^2/(1+4\eta^2)]^{1/2}} \quad (12)$$

$$\approx \left(\frac{\rho\tau_o H}{2p_4}\right)^{1/2}\frac{d\eta}{[\eta - \beta\eta^2]^{1/2}} \quad (12a)$$

where

$$\beta = 2(\tau_1/H)(K/p_4)$$

In general, $\eta \sim 0.1$–0.2 and Eq. (12a) is a good first approximation that has the advantage of being integrated to obtain an analytical expression

$$t_{\text{stretch}} = 2.54 \times 10^4(\rho\tau_o d/p_4\beta)^{1/2}\cos^{-1}(1 - 2\beta\eta_B)\mu\text{sec} \quad (13)$$

where ρ is in lb/in.^{3}, τ_o in inches, d is the diaphragm effective diameter in inches, and p_4 in pounds per square inches. The dimensionless fully stretched diaphragm height η_B is the height of the dome B divided by the diameter d after the diaphragm completes stretching and just begins to crack. η_B is determined experimentally from the diaphragms which have been subjected to static loading to burst.

Results

Equation (13) can be used to estimate the diaphragm stretch time with a knowledge of p_4, the diaphragm geometric characteristics, such as d, τ_o, τ_1, and its dynamic characteristic constants K and η_B.

Some experimental results on diaphragm stretch time were obtained from the UTIAS Implosion-Driven Shock Tube. This UTIAS facility consists of an 8-in.-diam hemispherical implosion driver chamber and a 1-in.-diam shock-tube channel separated by a 1-in.-diam stainless steel-scribed diaphragm. The diaphragms were machine scribed by a sharp mill cutter forming two right-angled grooves passing through the center.

Details of the operation of the UTIAS implosion driver are given in Ref. 8. Briefly, a detonation is generated in a stoichiometric hydrogen-oxygen mixture at the geometric center of the hemispherical driver chamber by an exploding wire. The hemispherical detonation wave moves towards the periphery and reflects from a shell of PETN explosive thus initiating the detonation of the explosive which drives an implosion towards the origin where the diaphragm is situated. In order to maximize the channel-shock velocity, it was necessary to allow the diaphragm to open before the arrival of the implosion.

It was shown[8] that the base pressure on the diaphragm increases rapidly from the initial loading value of 400–800 psi after the initiation of the detonation of the $2H_2 + O_2$ mixture and after a short ($\sim$4 μsec) period of overshoot it settled to a nearly constant value before the arrival of the implosion. The diaphragm undergoes stretching to burst then starts petaling open under this base pressure, p_4. The value for p_4 was found[8] to be very close to 6.7 times the initial loading pressure.

Table 1 Values of height of statically ruptured diaphragm with τ_o = 0.029 in. and different values of τ_1

τ_1 (in.)	0.014	0.016	0.018	0.020	0.022
$\eta_B = B/d$	0.15	0.19	0.23	0.28	0.33

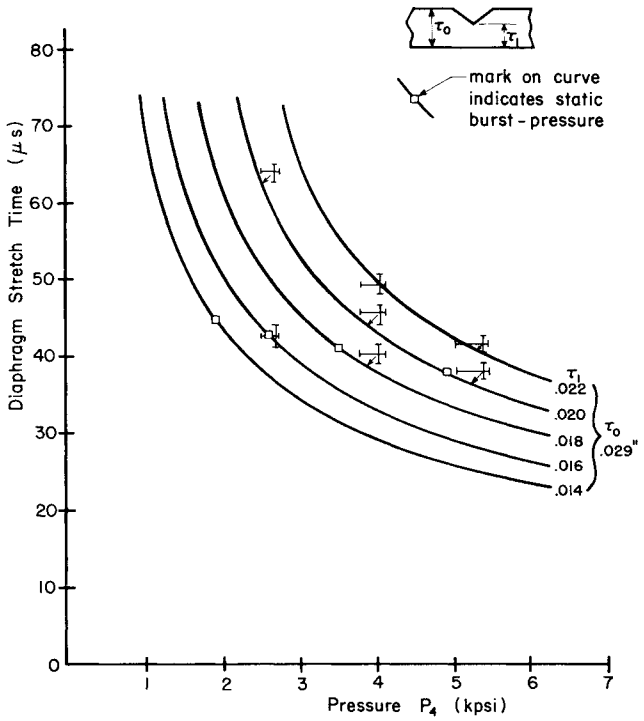

Fig. 2 Comparison of the predicted and the measured diaphragm-stretch time.

The diaphragms used in the experiment had a basic thickness (τ_o) of 0.029 in. and different scribed thicknesses (τ_1). The diaphragms were calibrated by subjecting them to static loading to burst. The corresponding values of η_B are shown in Table 1 for different values of τ_1. The diaphragm material was type 304 stainless steel which has a static stress-strain relationship $\sigma = K\varepsilon^n$ in the plastic range with $K = 9.4 \times 10^4$ psi and $n = 0.262$ at room temperature as obtained from tensile test data in Ref. 9. This value of K was used in Eq. (13). The material density ρ is 0.29 lb/in.^{3}.

Stretch times determined from Eq. (13) are plotted in Fig. 2 as a function of p_4 for different values of τ_1. Open squares on the curves indicate the static bursting pressure of the corresponding diaphragm. Shown in the same figure are a number of experimental points. The experimental data were obtained by monitoring the opening of the diaphragm with the use of a telescope focusing the diaphragm image onto a photomultiplier. The time lapse between the initiation of the gas detonation and the first detectable light signal was taken as the stretch time of the diaphragm.

Experiments were carried out at initial loading pressures of 400, 600, and 800 psi. The corresponding diaphragm base pressure p_4 was estimated to be 6.7 times the initial loading value. The agreement between theory and experiment is very good considering the simple model used. Notice that for $\tau_1 = 0.022$ in the static bursting pressure is higher than 7×10^3 psi (the point is off the graph). However, the diaphragm was still able to burst at a much lower (about 5200 psi) base pressure in the experiment. This suggests that the material does behave plastically under the present conditions. Experiments[8] also showed that maximum shock velocities could be obtained as long as the diaphragm began to burst at a time between a half to two-thirds the total time that it takes the implosion to reach the diaphragm.

References

[1] Glass, I. I. and Patterson, G. N., "A Theoretical and Experimental Study of Shock-Tube Flows," *Journal of the Aeronautical Sciences*, Vol. 22, 1955, pp. 73–100.

[2] White, D. R., "Influence of Diaphragm Opening Time on Shock Tube Flow," *Journal of Fluid Mechanics*, Vol. 4, 1958, pp. 585–599.

[3] Simpson, C. J. S. M., Chandler, T. R. D., and Bridgman, K. B., "Measurements of the Opening Times of Diaphragms in a Shock Tube and the Effects of the Opening Process on Shock Trajectories," Aero Rept. 1194, 1966, National Physical Lab., Teddington, Middlesex, England.

[4] Drewry, J. E. and Walenta, Z. A., "Determination of Diaphragm Opening-Times and Use of Diaphragm Particle Traps in a Hypersonic Shock Tube," TN 90, 1965, University of Toronto, Institute for Aerospace Studies, Toronto, Canada.

[5] Kirev, V. T., "On Motion of a Shock Wave During Non-instantaneous Opening of Diaphragm in Shock Tube," *News of Academy of Science USSR, Technology Section, Mechanics and Mechanical Engineering*, No. 6, 1962, pp. 144–146.

[6] Sandeman, R. J. and Allen, G. H., "A Double Diaphragm Shock Tube for the 10–20 km/sec Range," *Proceedings of the Eighth International Shock Tube Symposium*, edited by J. L. Stollery, A. G. Gaydon, and P. R. Owen, Chapman and Hall, London, England, 1971.

[7] Glass, I. I., Chan, S. K., and Brode, H. L., "Strong Planar Shock Waves Generated by Explosively-Driven Spherical Implosions," *AIAA Journal*, Vol. 12, No. 3, March 1974, pp. 367–374.

[8] Chan, S. K., "An Analytical and Experimental Study of an Implosion-Driven Shock Tube," Rept. 191, 1973, University of Toronto, Institute for Aerospace Studies, Toronto, Canada.

[9] Weiss, V., ed., *Aerospace Structural Metals Handbook, Vol. 1: Ferrous Alloys*, Syracuse University Press, Syracuse, N.Y., 1963.

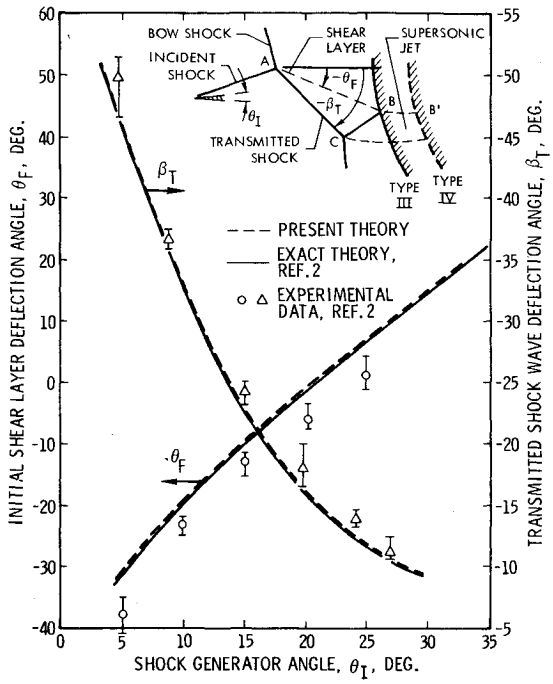

Fig. 1 Initial shear layer and transmitted shock deflections for $M_\infty = 6$, $\gamma = 1.4$.

Simple Technique for Predicting Type III and IV Shock Interference

T. Taz Bramlette*
Sandia Laboratories, Livermore, Calif.

THE problem of shock interference has been the subject of several recent experimental and theoretical investigations.[1–4] These references present theoretical methods for predicting the six types of interference observed by Edney[1] and suggest empirical correlations[1–3] for computing the heat transfer associated with each type of shock pattern.

The exact computation requires iterative solutions of the Rankine-Hugoniot relations. Since, in general, this requires a computer and under certain conditions (e.g., if trajectory calculations are desired) may involve considerable computing time, rapid approximate techniques are desirable. One such approach was recently suggested by Crawford,[4] who presented a clever graphical technique for predicting all six types of interference.

The purpose of the present Note is to describe an approximate method (based in part on a suggestion by Edney[5]) for computing both Type III and IV interference (see Fig. 1) and for predicting when the transition from one to the other occurs. These two interference patterns are of particular interest, since they may lead to the most severe shock interference heating problems.

Type III and IV interference patterns result from the intersection of an impinging weak oblique shock wave with a strong bow shock (Point A in Fig. 1). A shear layer emanates from this point which may impinge on the body (Point B) that generated the original strong bow shock (Type III interference), or it may form the first part of a more complex interaction which results in the formation of a thin, supersonic jet which impinges on the body at Point B′ (Type IV interference). If Type IV interference occurs, then the Point C intersection is similar to that at Point A; if Type III occurs, this intersection is more complex than schematically illustrated here, but the characteristics of the impingement Point B are independent of this detail. Whether Type III or IV interference occurs depends upon the angle between the shear layer AB and the surface tangent to the body at Point B.

The exact calculation for all six types of interference is described in detail in Ref. 2, which also contains computer program listings for each type. For Type III or IV the complete interference flowfield may be calculated if the freestream Mach

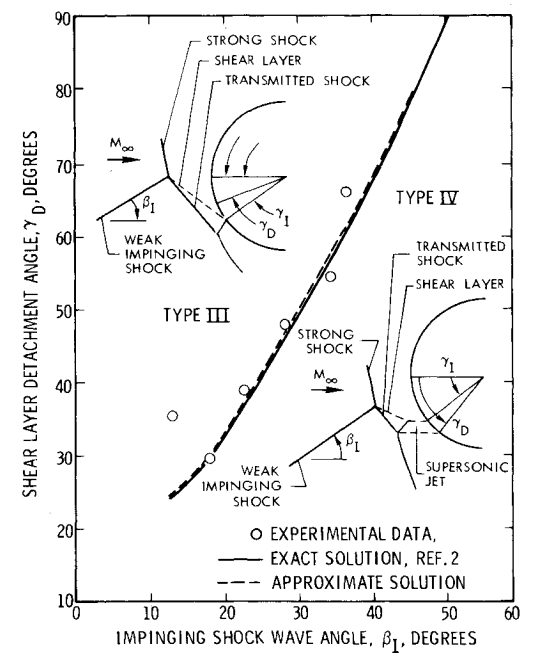

Fig. 2 Shear layer impingement angle for transition from Type III to Type IV interference for $M_\infty = 6$, $\gamma = 1.4$.

Received January 2, 1974; revision received February 23, 1974. This work was supported by the U.S. Atomic Energy Commission.

Index categories: Jets, Wakes and Viscid-Inviscid Flow Interactions; Shock Waves and Detonations; Supersonic and Hypersonic Flow.

* Member of Technical Staff. Member AIAA.